Available online at www.sciencedirect.com
ScienceDirect
Energy Procedia 2 (2010) 79–89
Energy Procedia
www.elsevier.com/locate/procedia

Spring Meeting

Structural and Morphological studies of $CuIn_{(1-x)}Al_xS_2$ deposited by spray on various substrates

N. Jebbari[a,a], B. Ouertani[b] , M.Ramonda[c], C. Guasch[c], N. Kamoun Turki[a] and R. Bennaceur [a]

[a]*Laboratoire de Physique de la Matière condensée, Faculté des Sciences de Tunis, Tunis El Manar (2092) Tunisie*
[b] *Institut Supérieur des Sciences et Technologie de l'Environnement de Borj Cedria, BP 95, 2050 Hammam-Lif. Tunisie*
[c]*Institut Electronique du Sud, Université de Montpellier II, Place Eugène BATAILLON 34 095 Montpellier cedex 05 France.*

Received 1 June 2009; received in revised form 1 December 2009; accepted 20 December 2009

Abstract

Structural properties of $CuIn_{(1-x)}Al_xS_2$ layers obtained by spray pyrolysis on various substrates were studied using X Ray Diffraction, Atomic Force Microscopy and Scanning electron microscopy. The concentration of Al in the spray solution, represented by the ratio z (z = $[Al^{3+}]/[In^{3+}]$), was varied from 0 to 3.2%. The different substrates are: glass, ZnO/glass, SnO_2/glass, ZnO/SnO_2/glass and In_2S_3/Glass. All the layers were deposited by spray. The ZnO used in the substrates was doped with indium. The concentration of indium in the ZnO sprayed solution is [In]/[Zn] = 3%.

The X-ray diffraction spectra revealed that, different values of the ratio z, the $CuIn_{(1-x)}Al_xS_2$ thin films were well crystallized in the tetragonal structure of the $CuInS_2$ material with the privileged orientation (112) whatever the substrate.

The surface topography of the $CuIn_{(1-x)}Al_xS_2$ thin films, deduced from the Atomic Force Microscopy, proved that the grain size in the top of the layers depends both on the z value and on the substrate.

The Auger analysis has been done in order to get information on the surface layer composition, the measurement show that the surface chemical composition where improved by annealing.

In this work the performances of the solar cell $CuIn_{(1-x)}Al_xS_2$(p)/$CuInS_2$(p)/In_2S_3(n)/ZnO, realized with optimized value of Al concentration, is also presented.

Keywords: Spray pyrolysis; $CuInS_2$ thin films; Grain size;

[a] Corresponding author. Tel.: +0-216- 98-474-281.
E-mail address: neila2410@yahoo.fr.

1876-6102
doi:10.1016/j.egypro.2010.07.014

1. Introduction

1.1. General introduction

$CuInS_2$ is one of the I-III-VI_2 semiconductor compound. Its direct band gap is about of 1.45 eV, which is close to the theoretical optimum for the conversion of the solar energy [1-3]. Furthermore, the $CuInS_2$ does not contain any toxic constituents, which makes it suitable for photovoltaic applications. In this work, $CuInS_2$ layers were prepared by Chemical Spray Pyrolysis (CSP) technique, which is an inexpensive method, non toxic and easy to manipulate. CSP is an attractive technique because a large-area film can be grown with good uniformity at low cost. The structural and optical [4] properties of sprayed $CuInS_2$ films depend on the preparation conditions mainly substrate temperature, and the ratio of Cu/In in spraying solution [4-6]. At substrate temperature T=320°C, the optimal composition of the pulverization aqueous solution was [5, 6]: 3.3×10^{-2}M of copper indium, 3×10^{-2}M of indium chloride and 12×10^{-2}M of Thiourea.

The introduction of aluminum in the spraying solution, in case of $z=[Al^{3+}]/[In^{3+}]=6\%$, improves the optical properties of the material[7,8].

In this work the effect of the aluminum concentration in spray solution is studied from 0 to 3.2%. The effect of the substrate on the compound structure is also studied. The aim of this work is to realize a solar cell with optimized optical and structural properties.

1.2. Experimental details a

Thin films are prepared by the pulverisation technique in liquid phase (spray). See Tab.1 for details concerning solution preparation. The experimental setup used to spray thin layers involves a heating system for the substrate, a nozzle fixed on a two-dimensional moving table allowing to pulverize the whole isothermal zone containing the heated substrates.

	Value or suitable item			
Compounds	SnO_2:F	ZnO: In	In_2S_3:Al	$CuIn_2S_3$
Item Solvent	Methanol	1/3 Propanol-2 And 2/3 Be-distillate	Be-distillate water	Be-distillate water
Solution concentration		$[In^{3+}]/[Zn^{2-}]=3\%$	$[In^{3+}]/[S^{2-}]=0.50$	$[Cu^{+}]/[In^{3+}]=z$
Precursors	$SnCl_4$	$(CH_3CO_2)_2Zn_2H_2O$	$InCl_3$ $SC(NH_2)_2$	$CuCl_2$ $SC(NH_2)_2$
Carrier gas	Compressed air	Compressed air	Nitrogen	Nitrogen
Distance sample-Nozzle	25 cm	25 cm	30 cm	30 cm
Rate of spray	20 ml/min	20 ml/min	5 ml/min	5 ml/min
Time of spray	5 min	30min	30-60 min	5 min

Table1: Spray parameter of each compound

The layer structure is studied by X-ray diffraction (XRD), using an automated Bruker D8 advance X-ray diffractometer with CuKα radiations for 2θ values over 20–60°. Respectively the wavelength, the accelerating voltage and the current were 1.5418Å, 40kV and 20mA respectively.

The film surface morphology is studied using a JEOL 6300F scanning electron microscopy (SEM). Auger measurements are carried out with a Riber system equiped with a cylindrical mirror analyser (CMA) and working on the first derivative mode. AFM is carried out with a Veecoo Dimension 3100 Atomic Force Microscopy using tapping mode.

1. Structural study

1.1. Substrate temperature effect

2. X-Ray diffraction spectra of undoped $CuInS_2$ Layer deposited on glass are presented in fig1 for different values of the substrate temperature T. It appears that a good crystallization of $CuInS_2$ thin films is achieved for all tested temperatures.

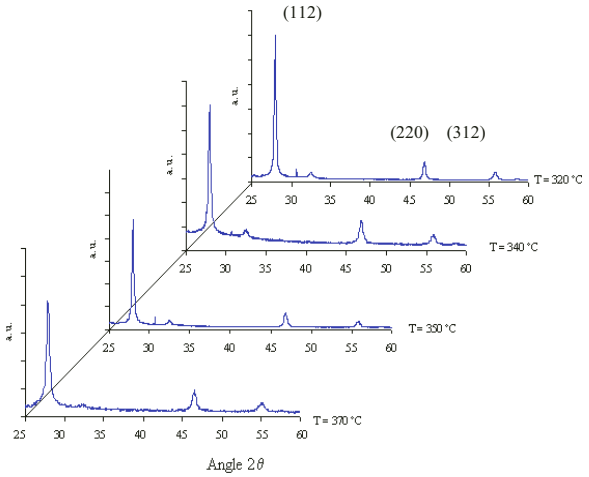

Fig.1. X-Ray Diffraction of $CuInS_2$ grown on Glass substrate at different temperatures.

The preferential orientation of $CuInS_2$ layers is (112) in the tetragonal structure. A zoom on this peak allows to show that the a good crystallization is obtained for all the substrate temperature range of [320°C - 370°C].

1.2. Role of the aluminum concentration ratio

XRD spectra of $CuIn_{(1-x)}Al_xS_2$ deposited on glass substrate at Ts=370ºC for different values of aluminum concentration in the sprayed solution are shown in Fig.3. it appears that these thin films are well crystallized according to the main orientation (112) for all the tested z values. The XRD patterns show that if the aluminum concentration in the spray solution increases from z=0% to z=3.2%, the intensity of (112) peak of $CuIn_{(1-x)}Al_xS_2$ varies and reaches a maximum value for z=0.11%.

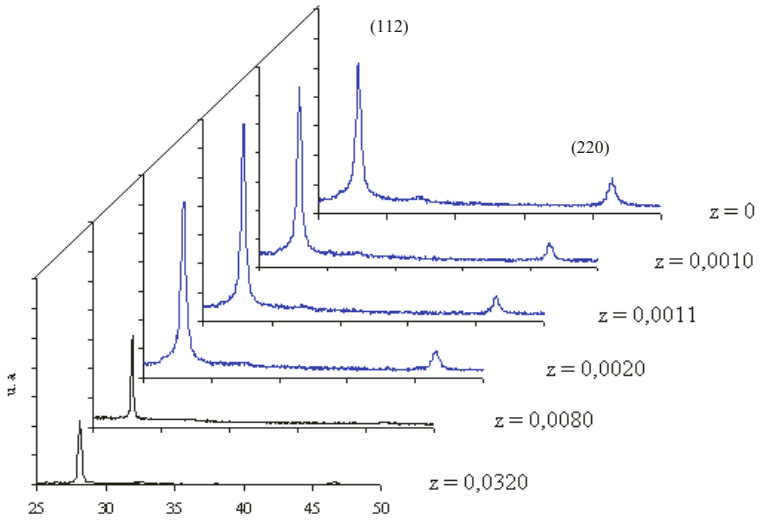

Fig.2. X ray diffraction of the $CuIn_{(1-x)}Al_xS_2$ deposited on glass substrate and achieved for different aluminum concentration in the solution (z=0, z=0.1%, z=0.11%, z=0.2%, z=0.8% and z=3.2%).

From these results it seems that the introduction of important concentration of Al in the prepared solution would increase the amorphous phase and would decrease the crystalline one.

For z ratio equal to zero the maximum of this peak intensity is measured for angle 2θ= 27.81°. If the concentration of Aluminum in solution increases, the value 2θ increases to 2θ= 27.90° for z=0.8% and to 2θ=28.12 for z=3.2%. This means that according to Bragg's low, the crystal of $CuIn_{(1-x)}Al_xS_2$ has a smaller lattice constant than $CuInS_2$. In fact, the aluminum atoms substitute to the indium ones which have a greater atomic radius (R_{In}: 1.626 A°, R_{Al}: 1.432 A°).

A zoom of the (112) preferential orientation peak is presented on Fig.4 for different Al concentration.

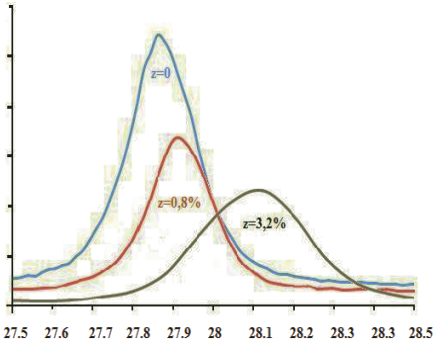

Fig.3. XRD spectra of (112) preferential orientation peak of the $CuIn_{(1-x)}Al_xS_2$ layer deposited on glass substrate and for different aluminum concentrations.

The full width at half maximum (FWHM=b_i) of the peak, increases from b_1=0.19°at z=0 to b_2=0.32° at z=3.2%. The crystallite size, *d*, is calculated using the Scherrer formula $d_i=k\lambda/(b_i \cos\theta)$, where λ is the X-ray wavelength (λ=1.54A°) and k=0.89 the Scherrer constant. The estimated values of grain size 125nm at z=0 and 36 nm at z=3.2%. So the grain size decreases when the Al concentration increases.

1.3. Substrate effect

Substrates were prepared by spray. The ZnO/In [9] film is crystallized in the hexagonal structure; main orientations are (101), (100) and (110), with (101) direction as the preferential one. SnO_2 and In_2S_3 layers exhibit good crystallization with the preferential direction of SnO_2 is (200) and the dominant one of In_2S_3 is (400) in the cubic structure [10].

1.3.1. Undoped CuInS2

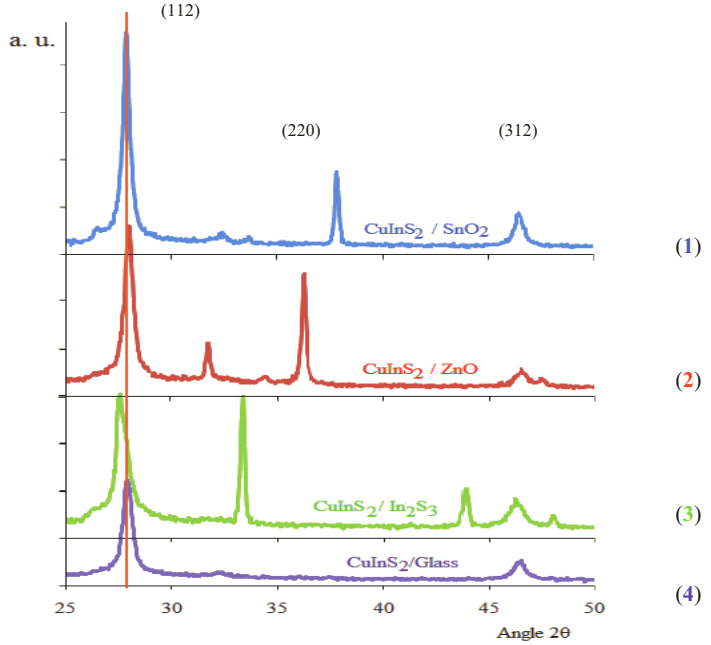

Fig.4. X ray diffraction spectraof $CuInS_2$ deposited on Glass, In_2S_3/glass, ZnO/Glass and SnO_2/Glass, achieved for substrate temperature equal to 320 ºC. The layers were deposited on the different substrates at the same time.

Fig.4 compares the growth of $CuInS_2$ thin films deposited on Glass, Indium sulfide In_2S_3/Glass, ZnO/Glass and SnO_2/Glass substrates. An increase of the intensity of the main DRX peak of the $CuInS_2$ is observed as the substrates goes respectively from SnO_2/glass(4), ZnO/glass(3), In_2S_3/glass(2) and glass(1).

One can observe that the maximum of intensity is measured at the same value of angle value if the substrates are SnO_2/glass and glass. If the substrate is In_2S_3/glass the maximum of intensity is measured at angle value. For ZnO/glass substrate the maximum intensity is measured at angle value. This small shift is due to stress in the layer, which depends on the substrate. According to Bragg's law, the $CuInS_2$ layer is extended when deposited on ZnO.

1.3.2. Substrate effect for doped $CuInS_2$:Al with z=3.2%

Fig.5 compares the growth of $CuIn_{(1-x)}Al_xS_2$ thin films deposited on zinc oxide (ZnO) and glass substrates. DRX spectrum of the ZnO layer is given as reference. The ratio of concentrations of aluminum and indium in the solution is z =3,2%. Fig.5.c shows the peaks (100), (101) and (110) relative to the zinc oxide. The (101) direction is the preferential one. The ZnO film is crystallized in the hexagonal structure. Fig.5.b shows the peak corresponding to the main orientation (112) of the $CuIn_{(1-x)}Al_xS_2$ phase in the tetragonal structure. A clear reduction of the intensity of the peak of the $CuIn_{(1-x)}Al_xS_2$ is observed when the glass substrate is swapped with the ZnO one.

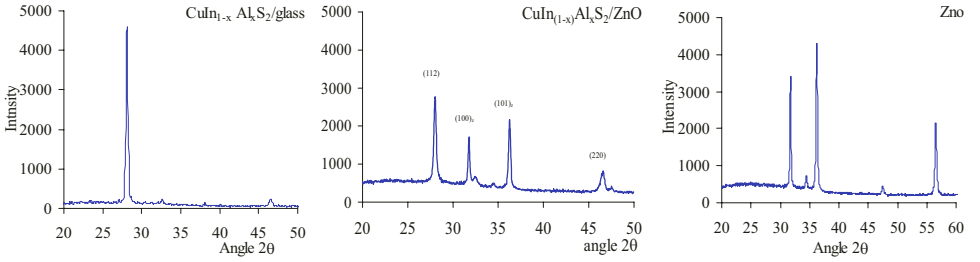

Fig.5 : XRD spectera of $CuIn_{(1-x)}Al_xS_2$ / glass (a), $CuIn_{(1-x)}Al_xS_2$/ZnO/glass (b) and ZnO / glass (c), achieved with aluminum concentration in the solution equal to 3,2% and for substrate temperature equal to 320 ºC.

Fig.6 shows DRX spectrum obtained on $CuIn_{(1-x)}Al_xS_2$ thin films deposited on tin oxide (SnO_2). DRX spectrum of the SnO2 layer is given as reference (fig.6b). The (110) and (200) peaks corresponding to tin oxide substrate is observed. The main orientation (112) of the $CuIn_{(1-x)}Al_xS_2$ material in the tetragonal structure is clearly visible. However a clear reduction of the peak intensity of the $CuIn_{(1-x)}Al_xS_2$ is observed as the glass substrate is swapped with the ZnO one. The order of the reduction can be deduced from the ratio of intensity.

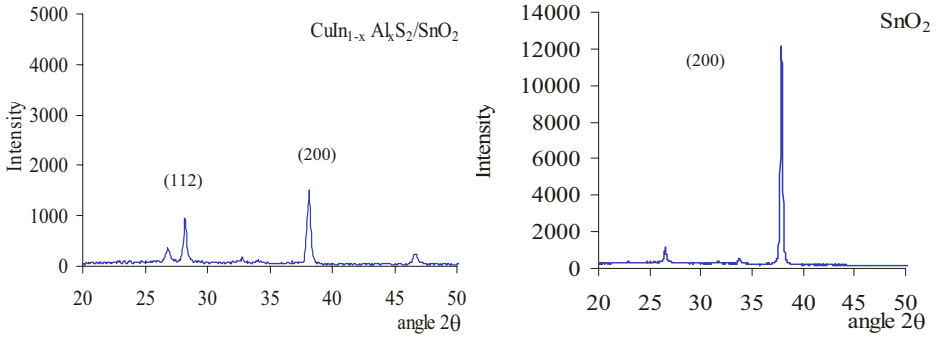

Fig.6 : XRD spectra of $CuIn_{(1-x)}Al_xS_2/SnO_2$/Glass (a) and SnO_2/ Glass(b), achieved for report of the aluminum and indium concentrations in the solution equal to 3,2% and for substrate temperature equal to 320 ºC.

From this result, we deduced that the crystal properties of the $CuInS_2$:Al layer is less affected by the ZnO substrate than the SnO_2.

2. Surface Morphology

2.1. Role of the aluminum concentration

A.F.M images of $CuIn_{(1-x)}Al_xS_2$ layer deposited on glass is presented on fig.7 and 8. For z=0, crystallites can be identified. They exhibit elongated shape with grain size ranging from have 100 to 215nm, which is comparable to the estimated value 125nm obtained from DRX spectra (see pragraph2.2). The variance of height distribution (RMS roughness) is 1,220nm..

If z=3.2%, the crystallites have spherical form and uniform distribution. Their size is smaller, in the range between 20 to 67nm, which is also comparable to DRX result. The RMS Roughness is 1,530nm in this case.

One can conclude that the introduction of aluminum in the thin film of $CuInS_2$ decreases grain size and increases surface roughness. Aluminum is very reactive with the oxygen; its presence reduces the mobility of atoms at the surface. These observations can inform us on the nucleation process during the growth. It appears necessary to reduce the Al concentration as much as possible. The amount z=0,11% could be the optimum percentage as shown above in Fig3.

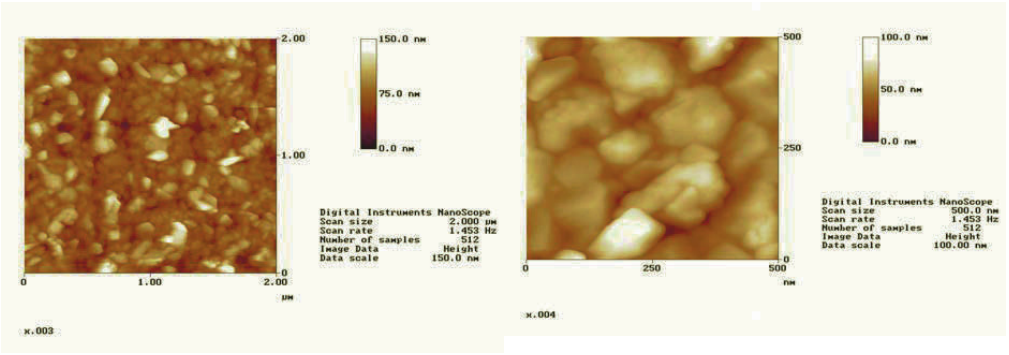

Fig.7. Surface topography of undoped $CuInS_2$ layer deposited on Glass at Ts=320ºC.

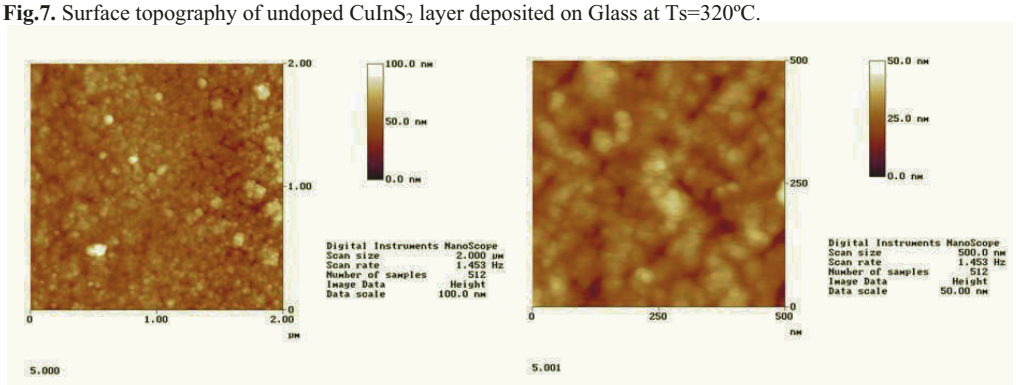

Fig.8. Surface topography the $CuIn_{(1-x)}Al_xS_2$ layer deposited on Glass at Ts=320ºC and achieved for aluminum concentration in the solution z=3.2%.

2.2. Role of surface morphology of substrates

Surface morphology of the $CuInS_2$ films deposited on glass is investigated by Scanning Electron Microscopy (SEM)and presented in (Fig.9). The surface of the film appears foliated Fig. 9.a). The SEM cross-section view

(Fig.9.b) shows that the as-prepared film has a good adherence. The average value of the thickness is estimated to about 300 nm. The same foliated morphology is shown by the In_2S_3 layer deposited on glass (Fig.10.a1). The cross-section SEM image of the In_2S_3 layer deposited on glass (Fig.10 a2) exhibits a good adherence but a tubular growth. The thickness of this In_2S_3 layer is estimated to 2300nm.

Surface morphology of the ZnO film deposited on glass was appears granular (Fig. 10 (b1)). The SEM cross-section view (Fig.10.(b2)) shows that the ZnO film has a good adherence. The average value of the thickness is estimated to 1000 nm. A granular morphology is also observed at the surface of the SnO2 deposited on glass (Fig.10c1).The cross-section shows a good adherence of the SnO2 layer (Fig.10c2) and the film thickness is estimated to 1000nm.

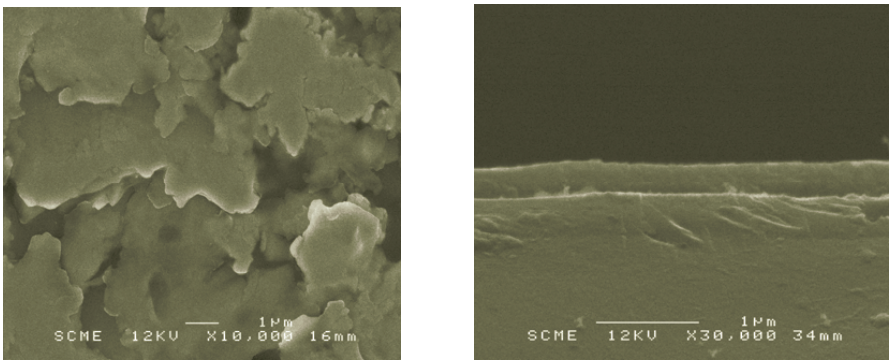

(a) (b)

Fig.7. SEM image of the $CuInS_2$ layer deposited on glass ((a) surface, (b) cross section)

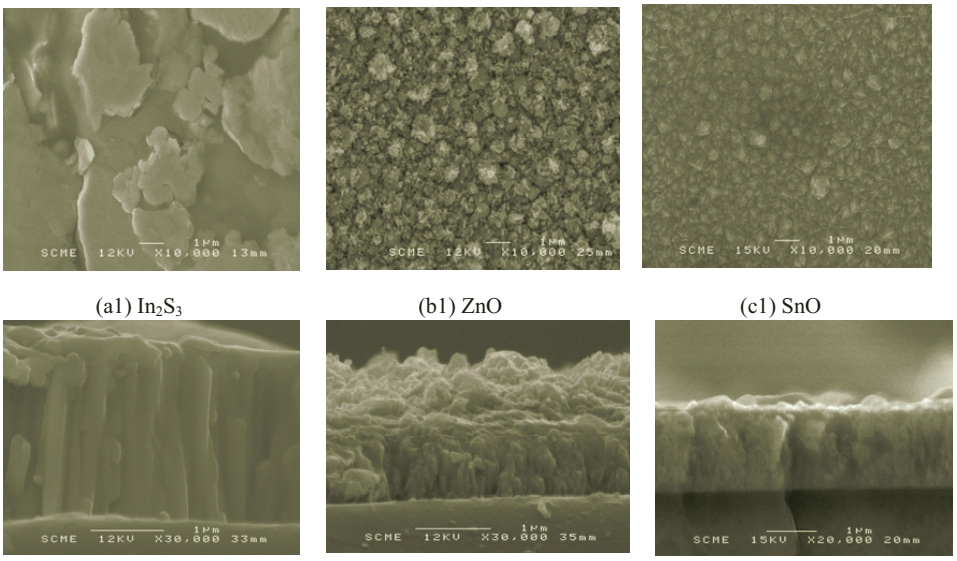

(a1) In_2S_3 (b1) ZnO (c1) SnO

(a2) (b2) (c2)

Fig.8. SEM image of the In_2S_3, ZnO and SnO2 layers deposited on glass ((1) top view, (2) cross section)

3. Chemical analyses of the $CuInS_2$ thin film

3.1. Surface composition

The Auger spectroscopy has been performed in order to gather information on the surface layer composition of the $CuInS_2$ thin film.

The first step of this work concerned the surface composition homogeneity. In order to check this homogeneity, we selected several points on the surface and we plotted Auger spectra for each of them. These spectra being similar, we concluded that the surface homogeneity was good at the scale of the Auger measurements accuracy. Spectra are characterized by the presence of the constituent elements Cu, In, and S, as well as Cl, as inert residue of the chemical spray solution. As expected, C and O are also detected, as impurity elements adsorbed in the surface layer. The oxygen may be incorporated into the film either from the atmosphere or from the aqueous solutions sprayed to form the CuInS2 thin films. The source for carbon contamination may be due to the exposure of the samples to atmospheric air, and to the laboratory environment in which samples are manipulated. Substrate and Aluminum concentration influence surface composition of the $CuInS_2$:Al layer. As shown in Table2. The surface composition, after annealing $CuInS_2$ thin films grown with different aluminum doping rate (Al/In =1‰, 1.1‰ and 2‰), are reported in Table3.

z	0		1‰	2‰	8‰	3.2%		
Substrates	Glass	SnO_2	Glass	Glass	Glass	Glass	SnO_2	ZnO
H(Cu)/H(In)	0,72	0,98	0,443	0,258	1,18	0,198	0,826	0,429
H(S)/H(In)	0,09	0,203	0,095	0,153	-----	0,21	-----	0,062
H(Cl)/H(In)	0,041	0,045	0.059	0,092	-----	0,13	-----	-----
H(O)/H(In)	2,345	2,223	1,551	1,634	2,35	3,36	3,29	2,28
H(C)/H(In)	1,67	1,34	0,781	1,909	1,16	3,9	1,9	1,05

Table2: Surface composition of thin layer of $CuIn_{(1-x)}Al_xS_2$ deposited on different substrates and for varied values (z) of aluminum concentrations in the spray solution.

z	1‰	1,088‰	2‰
Eléments	$CuIn_{(1-x)}Al_xS_2$	$CuIn_{(1-x)}Al_xS_2$	$CuIn_{(1-x)}Al_xS_2$
H(Cu)/H(In)	2.065	0.82	2.012
H(S)/H(In)	2.793	1.06	1.659
H(Cl)/H(In)	0.27	0.130	0,200
H(O)/H(In)	1.329	1,734	1.967
H(C)/H(In)	12.566	7.513	8.18

Table3: Surface composition of thin layer of $CuIn_{(1-x)}Al_xS_2$ deposited on Glass and for varied values (z) of aluminum concentrations in the spray solution after annealing.

3.2. Volume composition

Measurements of the atomic concentration are taken for different position of the sample by EDS. The average value in atomic percent of each element is presented in table4 for z=0 and z=0.1%. The average value is around of stochiometer values.

	Al	C	O	S	Cu	In	S/In	Al/In	Cu/In
CuInS2	0	17,18	0	29,14	17,05	12,65	2,30	0	1.35
CuInS2:Al(1â)	0	8,67	45,29	18,18	9,10	7,79	2,33	0	1.16

Table4: EDS analyses of $CuIn_{(1-x)}Al_xS_2$ layer obtained with varied concentrations (z) in the spray solution.

4. Solar cell

The results presented in the following part concern an heterostucture that exhibit maximum of open circuit voltage value among a series of heterostructures fabricated with various doping levels of the In_2S_3 layer. Moreover, combination of CuInS2:Al with CuInS2 allows to make thicker layer, due to good coherence between CIS:Al and undoped CIS. This will be extensively published in a forthcoming paper.

The electrical properties of the photovoltaic structure $CuInS_2$:Al (p)/ $CuInS_2$ (p)/In_2S_3(n)/ZnO with x=0.22 are studied by I(v) measurements (Fig.12).

Characteristic deduced from these curves are summarized in table4. They show a good Vco but the Icc is very low. This is due to fissuring at the grain boundaries of $In_{2-x}Al_xS_3$ layer (Fig.11a1). In future work we wish to eliminate this stress by using Pyrex substrate. Surface morphology and depth profile of solar cell compounds is represented in fig.9.

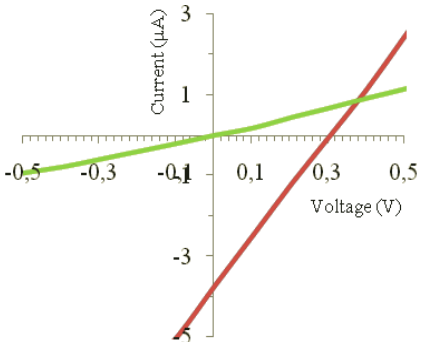

Fig.8: I (V) patterns of solar cells, $CuInS_2$:Al (p)/ $CuInS_2$ (p)/In_2S_3(n)/ZnO:In.

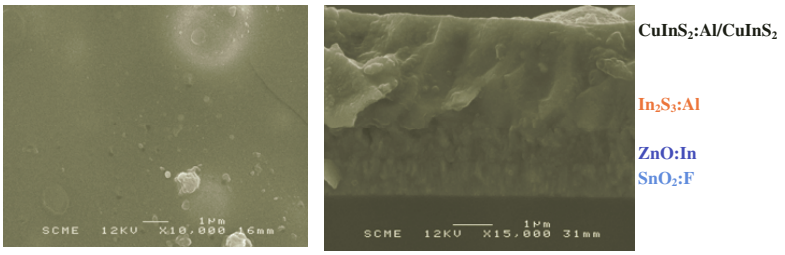

Fig.9. Surface morphology and depth of solar cell compounds.

Jcc	Vco	FF	Rs	Rsh	Iph	Is
0.52 µA/cm^2	380mV	0.25	6.55 kΩ	9 kΩ	5µA	5 µA

Table4: Characteristic quantities of the solar cells prepared from the CIS sample.

5. Conclusion

The obtained results confirm that the nature and the structure of the substrates have a great effect on the growth of the $CuInS_2$:Al layer and on the preferential orientation of this films. Stress of opposite signs appears when $CuInS_2$ is deposited on ZnO or on In_2S_3. There is a good agreement between XRD and AFM results concerning grain size determination. The presence of Al atoms in the $CuInS_2$:Al material noticeably modifies to the growth and the structure of the film. The $CuInS_2$:Al layer exhibits maximum grain size and crystallization when z<0.2%. Above this Al concentration, an alloy is formed $CuIn_{(1-x)}Al_xS_2$ with smaller grains.

We have investigate the electrical properties of the heterostructure $CuInS_2$:Al (p)/ $CuInS_2$ (p)/In_2S_3(n)/ZnO:In fabricated as an example of solar cell, with ptimized growth conditions for the $CuInS_2$:Al layer. The open circuit voltage is relatively comparable with the state of the art solar cells. The other electrical parameters should be optimized with a better control of the grain size and preferential orientation of each layer.

Acknowledgments:
The authors wish to thank the ComitÈ Mixte de Cooperation Universitaire As well as Egide France for financial support under the project number 07S/1304.

References

[1]A. Werner, I. Luck, J. Bruns, J. Klaer, K. Siemer, and D. Braunig, Thin Solid Films **361**, 88 (2000).
[2]K. I. N. Matsumoto, T. Horiuchi, K. Ichino, H.Shimoyama, T. Ohashi, Y. Hashimoto, I. Hengl, J. Beier, R. Klenk, A. Jager-Waldau, and M. C. Lux-Steiner, Jpn. J. Appl. Phys. Part 1 **39**, 126 (2000).
[3]N. Kammoun, R. Bennaceur and J. M. Frigerio, J. Phys. III **4,** 983 (1994).
[4]M. Krunks, O. Bijakina, T. Varima and E. Millikov, Thin solid films **388**, 125 (1999).
[5]N. Kammoun, S. belgasem, M. Dachraoui and R. Bennaceur, Rev. Phys. Appl. **22**, 991 (1987).
[6]N. Kammoun, S. belgasem, M. Amlouk, R. Bennaceur, K. Abdelmoula and A. Belhadj Amara, J. Phys. III **4,** 473 (1994).
[7]N. Kammoun, N. Jebbari, S. belgasem, and R. Bennaceur, J. Bonnet, F. Touhari and L. Lassabatere J. Appl. Phys. **91**, 4 (2002).
[8]N. Kamoun Allouche, N. Jebbari, C. Guasch, N. Kamoun Turki, 23nd European Photovoltaic Solar Energy Conference, 2008, Germany.
[9]M.Amlouk, F.Touhari, S.Belgacem, N.Kamoun, D.Barjon, and R.Bennaceur, Phys. Stat. sol 73, (1997).
[10]N. Jebbari, N. Kamoun, C. Guasch and R. Bennaceur, 22nd European Photovoltaic Solar Energy Conference, 3-7 September 2007, Milan, Italy.